Thermal effects of copper-graphene composite films in a human skin analogous for the application to clothing

Yelin Ko
College of Human Ecology, Seoul National University, Seoul, Republic of Korea
Sora Shin
College of Human Ecology, Seoul National University, Seoul, Republic of Korea and Graduate School of Design, Kyushu University, Fukuoka, Japan
Yong Seok Choi
Graphene Square Inc. and Graphene Research Center, Advanced Institute of Convergence Technology, Suwon, South Korea
Byung-Hee Hong
Department of Chemistry, Seoul National University, Seoul, Republic of Korea and Graphene Square Inc. and Graphene Research Center, Advanced Institute of Convergence Technology, Suwon, South Korea
Sang-Yoon Park
Nano-Bio Research Laboratory, Advanced Institute of Convergence Technology, Suwon, South Korea, and
Joo-Young Lee
College of Human Ecology, Research Institute of Human Ecology, Seoul National University, Seoul, Republic of Korea

Received 31 October 2019
Revised 21 January 2020
Accepted 27 January 2020

Abstract

Purpose – The purpose of the study was to explore heat-accumulative and thermal-conductive characteristics of copper-graphene composite film (Cu-G film) while applying it to a human-skin analogue.

Design/methodology/approach – In the preliminary experiment, the authors evaluated the thermal conductive characteristics of the Cu-G film in three covered conditions (no film, copper film, and Cu-G film conditions). For the first factorial experiment, the heat-accumulative properties over heated pig skin were compared at air temperatures of 10, 25 and 35°C. For the second factorial experiment, 105 trials were conducted on pig skin by combining air temperatures, trapped air volumes, and numbers of film layers.

Findings – The results from the preliminary experiment showed that the Cu-G film distributed the surface heat to the outside of the Cu-G film, which resulted in even distribution of heat inside and outside the Cu-G film, whereas the copper film accumulated heat inside the copper film. The human-skin analogue of pig skin, however, showed the opposite tendency from that of the plastic. The pig-skin temperatures beneath the Cu-G film were higher than those beneath the copper film, and those differences were remarkable at the air temperature of 10°C. The accumulative heat was affected by the trapped air volume, fit to the skin, and number of Cu-G film layers.

This research was supported by Nano-Material Technology Development Program through the National Research Foundation of Korea (NRF) funded by the Ministry of Science, ICT and Future Planning (No.2016M3A7B4910).

International Journal of Clothing Science and Technology
Vol. 32 No. 4, 2020
pp. 601-618

0955-6222
DOI 10.1108/IJCST-10-2019-0163

Originality/value – In conclusion, the Cu-G film more effectively accumulated heat on the human-skin analogue than copper film, and those effects were more marked in cold environments than in mild or hot environments.

Keywords Copper-graphene composite film, Thermal conductivity, Heat accumulation, Cold-protective clothing

Paper type Research paper

1. Introduction

Graphene is a single-atomic carbon layer of graphite discovered by Andre Geim and Konstantin Novoselov, who received the 2010 Nobel Prize in Physics for "Groundbreaking experiments regarding the two-dimensional material graphene" (The Nobel Prize, 2010). Graphene has exceptional electronic, mechanical, chemical, and thermal properties. In particular, graphene has the highest thermal conductivity among carbon materials, in the range of 3,000–5,000 $W \cdot m^{-1} \cdot K^{-1}$ at room temperature. Because of its exceptionally high thermal conductivity, a considerable amount of research on the thermal behavior of graphene has been conducted, but the most of this research focused on the thermal properties of small samples of graphene.

Since the synthesis of high-quality stretchable graphene films on a large scale became possible using the chemical vapor deposition (CVD) method (Bae *et al.*, 2010; Kim *et al.*, 2009), there have been robust efforts in applying graphene practically to exploit its exceptional properties. Compared with the studies carried out on the electronic (Ito *et al.*, 2018; Kim *et al.*, 2018b), biomedical (Kim *et al.*, 2018a), and energy storage (Mao *et al.*, 2018) applications of graphene, there have been relatively few studies on incorporating graphene into textiles and fabrics for its application to clothing. In this context, the thermal properties of graphene due to its high thermal conductivity are of particular relevance for thermoregulatory clothing. Clothing is more than "a passive cover for the skin" as it can interact with the heat control functions of the skin and as its effects are also influenced by thermal environments (Zhang *et al.*, 2002). Human body is surrounded by microclimate between clothing and the skin. Body heat exchange occurs through the surrounded environment with clothing. In thermal environments, graphene-incorporated clothing can provide efficient heat transfer from the skin to the ambient environment and can provide more insulation for the skin by reducing heat loss.

Graphene-based flexible heaters have been applied to wearable technologies and clothing. Lin *et al.* (2017) reported that silver-particle-mixed graphene increased up to 220°C within 5 s with uniform temperature distribution in its steady state and concluded that with its high steady-state temperature, ultrafast response, and excellent flexibility, a graphene heater had promising wearable applications. Shin *et al.* (2017) compared continuous and intermittent heating protocols using graphene flexible heater–incorporated clothing in a cold environment. They confirmed the practicality of a graphene heater for cold-protective clothing. Although active heating using graphene heaters has often been considered necessary for thermal management clothing, battery efficiency still constrains rapid development, especially for cold environments. The issue is that a smart wearable system must be lightweight in order not to impede movement yet also be able to provide lasting thermal protection. Providing maximal thermal protection against cold environments with limited battery capacity is especially important for workers who perform strenuous tasks in extreme cold and may have difficulties while charging batteries. Thus, increasing passive insulation using proper clothing material and enhancing battery efficiency are important.

To evaluate the thermal effects of large-scale graphene itself, and its applicability to clothing without any battery, it is necessary to understand the microclimate between the human skin (or human-skin analogue) and graphene. To the best of our knowledge, however, there have been no studies that investigated the thermal effects of graphene film on the human skin. Thus, we adopted pig skin as a human-skin analogue and tested it as part of a clothing microclimate

system to evaluate the thermal effects of copper-graphene composite films on the human skin. Bearing in mind human-skin temperature distribution and the cutaneous vascular system, both global and local skin surfaces were emulated with the human-skin analogue and the heating units. We chose a test method using the real pig skin and graphene film, rather than a theoretical test simulating based on physical laws, in order to explore possibilities for practical applications. We hypothesized that the copper-graphene composite film would show better thermal, conductive properties than those of the copper film and no film conditions.

2. Materials and methods

A copper-graphene composite film (Cu-G film) was synthesized by growing monolayer graphene on both sides of a high-purity copper film (Alfa Aesar, 99.99 percent) through a CVD method (Graphene Square Inc., Korea) (Lee *et al.*, 2016) (Figure A1). We chose Cu-G films in the present study because copper is the most commonly used catalyst for CVD graphene production. Three different experimental protocols were as follows: the first and preliminary experiment (Exp. 1) was formulated to reflect temperature variation of large three-dimensional surfaces, not a two-dimensional surface. The second experiment (Exp. 2) was designed to represent, with pig skin as a human-skin analogue, the temperature variation of the human skin with its cutaneous vascular systems. The third experiment (Exp. 3) was designed similar to the second one but with addition of air gaps between the skin and a clothing layer, on smaller surfaces. For all three experiments, copper film was compared with Cu-G film, and the no-film condition was used as a control condition (3 experiments × 3 experimental conditions).

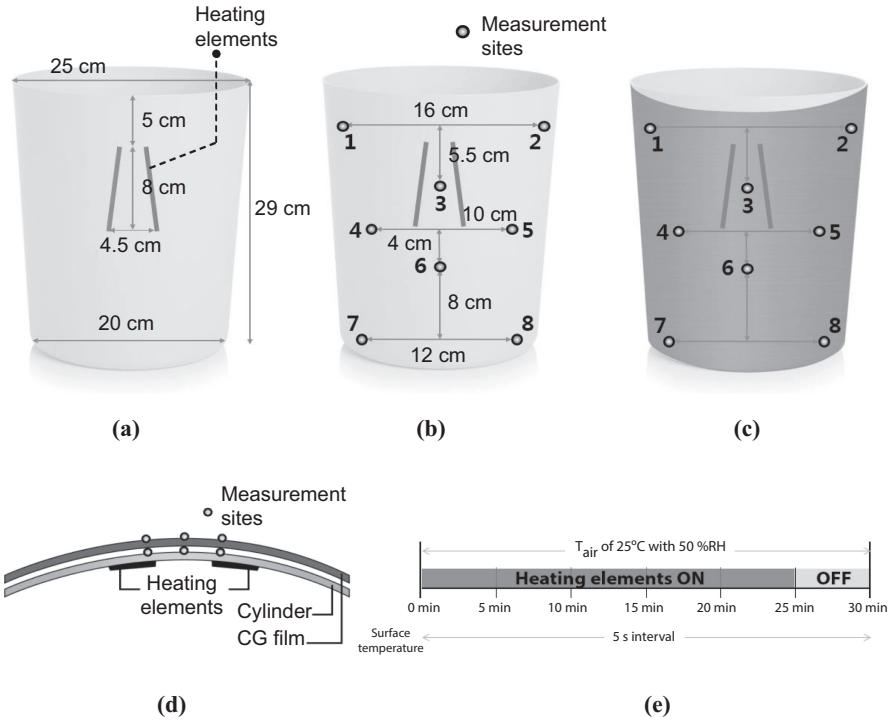

Figure 1.
[Exp. 1] Location of heating elements on interior surface of the cylinder (a), eight measurement sites of surface temperature of the cylinder (b), eight corresponding measurement sites of surface temperature of copper film or copper-graphene composite (Cu-G) film (c), experiment setup in a section view (d), and the experimental protocol (e)

2.1 Exp. 1: thermal effects of Cu-G films on the three-dimensional surface

Two heating elements (2.3 cm width and 8.0 cm length each, heating up to 200°C in 50 s) were perpendicularly attached to the interior surface of the polypropylene cylinder to reproduce temperature variation of the human skin (Figure 1a–c). For the Cu-G film and copper film conditions, each film (42 cm width × 30 cm length) was firmly attached to the exterior cylinder surface (Figure 1d). For the no-film condition (control), the cylinder surface was exposed to air without any film. Temperatures of the exterior surface of the cylinder and that of the films were measured on eight sites (Figures 1b and 1c). Middle sites, which were closest to the heating elements, consisted of sites #3, #4, #5, and #6 (MIDDLE). Sites #1 and #2 and #7 and #8 were grouped into UPPER and LOWER, respectively. All temperatures were measured with thermistor probes and recorded every 5 s using a data logger (LT-8A; Gram Corporation, Japan). Temperature data were then averaged into 5 min for analytical and graphical purposes. Each experimental trial consisted of 25 min of heating (heating elements on) followed by 5 min of no heating (heating elements off) at an air temperature of 25°C with relative humidity of 50 percent (Figure 1e).

2.2 Exp. 2: thermal effects of Cu-G films on a human-skin analogue with cutaneous vascular system

Pieces of pig skin (43 cm width × 22 cm length) were used as a human-skin analogue since pig skin is known to be anatomically and physiologically similar to the human skin and has been used as a human-skin analogue in other skin studies (Sullivan *et al.*, 2001). The pig skin used in the present study had a thickness of 2.0 ± 0.5 mm and a mass of 0.5 ± 0.1 g·cm^{-2}. The pig skin was kept in a freezer until 24 h prior to experimental trials and then kept in a refrigerator for 24 h. Hair was shaved if needed. Surface oil of the skin was removed with oil papers approximately 30 min before each trial started. Each pig skin was used only for one trial so that any possible protein or tissue modification induced by heat would not affect the results. A heating system consisting of seven copper pipes (40 cm length, 12 mm external diameter, and 11 mm internal diameter for each pipe) was developed to reproduce cutaneous blood flows underneath the skin (Figure 2a). Water flowing into one end of the silicone hoses and

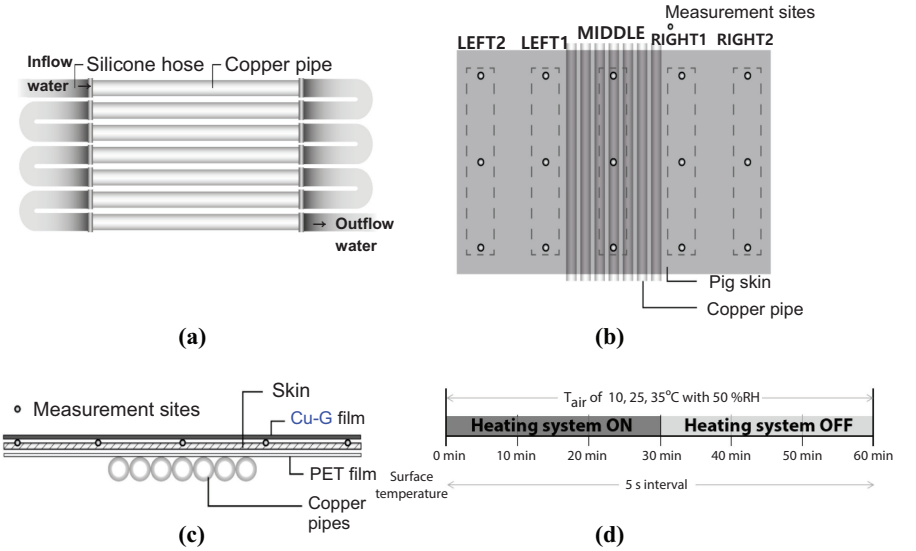

Figure 2.
[Exp. 2] A heating system with copper pipes and silicone hoses (a), 15 measurement sites in a plane view (b), experiment setup in section view (c), and the experimental protocol (d)

out to the other end of the hoses circulated with a water circulator (RW-0525G, JEIO TECH, South Korea). A layer of PET film was placed between the heating system and the skin to prevent the heating system from skin oil. Four Styrofoam sticks were attached to the four edges of the PET film so that it withstood the weight of the pig skin. The heating system was placed beneath the center of the skin so that heating was uneven so as to reproduce the overall temperature gradient of the human skin (Figure 2b). The large-scale Cu-G film (42 cm width × 30 cm length) covered the pig skin (Figure 2c). Experiments were conducted at air temperatures of 10, 25 and 35°C and 50 percent relative humidity.

The pig-skin temperatures underneath the films were measured on the 15 sites and grouped into five sections: LEFT2, LEFT1, MIDDLE, RIGHT1, RIGHT2, averaging the three measurement sites in the same column (Figure 2c). All temperatures were measured with the same thermistor probes and a data logger used in the experiment 1. Overall temperature distribution of the pig skin was visually expressed by plotting the temperature from the 15 skin sites using Origin 9.0. After 10 min of heating, the pig-skin temperatures of the heated MIDDLE section reached 33–34°C reproducing the mean skin temperature of the human body in comfort ranges (Parsons, 2014), measurements started. The water inflow temperatures of the heating system, which were decided by pretests, were set at 90, 70, and 60°C with the air temperatures of 10, 25, and 35°C, respectively. Each experimental trial lasted for 60 min. During the first 30 min, the heating system was turned on and maintained at the set temperature, then it was turned off for the last 30 min (Figure 2d).

2.3 Exp. 3: thermal effects of Cu-G films on a human skin and clothing analogue with air gaps

Small-scale Cu-G film (8 cm width × 8 cm length) or copper film covered the skin (10 cm × 10 cm) with trapped air on the middle of the skin (curved condition) mimicking an air gap between the skin and clothing or with no air (flat condition). Air gaps of four different volumes (3.9, 7.9, 17.7, and 23.6 cm^3 for V1, V2, V3, and V4, respectively) were formed using a semielliptical cylinder, which was manufactured using a 3D printer (Figure 3a and b). Rhino 5 was used for modeling these solids. Films having four different volumes were shaped by applying pressure to the films over the solid. For the curved condition, minimum of one layer

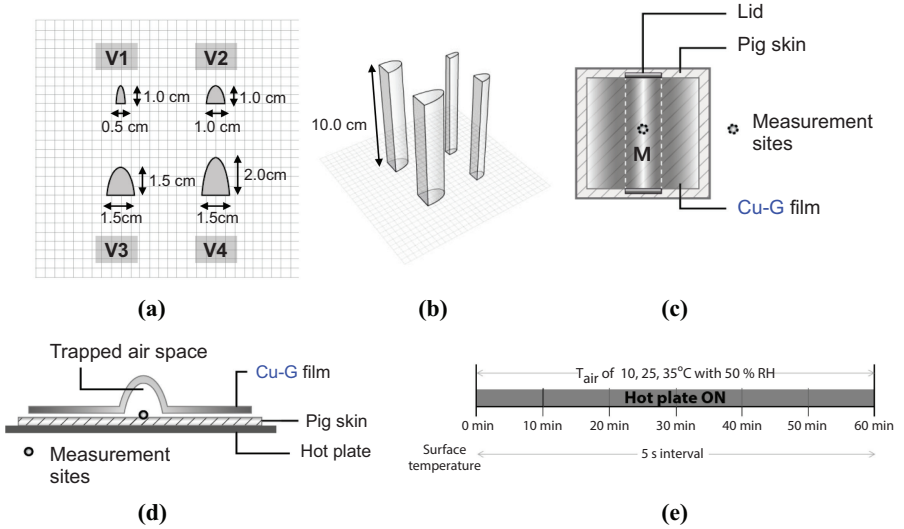

Figure 3.
[Exp. 3] Semielliptic cylinders with four different cross-sectional areas (a) and 10-cm height (b), experimental setup in a plan view (c), in a section view (d), and the experimental protocol (e). The volumes of the four cylinders are 3.9, 7.9, 17.7, and 23.6 cm^3 for V1, V2, V3, and V4, respectively

to maximum of four layers of CU-G or copper film (1, 2, 3, and 4L) covered the pig skin. For the multiple layered conditions, the film layers were stacked and shaped all together. The widths of the Cu-G and copper films were calculated for each air gap size, to make the air gap inside the film 8 cm × 8 cm when viewed from above. To form "closed" air gap between the skin and the film, both ends were covered by lids made of the same material as the film. The flat condition had one layer of Cu-G or copper film.

Experiment 3 consisted of a total of 105 combinations: film material (no film, copper film or Cu-G film), film shape (curved or flat surfaces), air gap volume (V1, V2, V3, or V4), the number of film layers (1, 2, 3, or 4L), and ambient temperatures (air temperatures of 10, 25, or 35°C) (3 film conditions × 2 surface conditions × 4 air gap conditions × 4 layer conditions = 96 conditions + 9 conditions) (Table I). Bottom of the pig skin was evenly heated for 60 min by a hot plate to simulate local human body human-skin temperature (Figures 3d and 3e). Thermistor probes were attached to the middle of the pig skin to monitor skin temperature (Figure 3c). Hot plate (DH.WHP03024, DAIHAN Scientific, Korea) temperatures were set according to the three different levels throughout the experimental period to enable the skin temperature to stabilize for the first 10 min: 46, 38, and 35°C at T_{air} of 10, 25, and 35°C, respectively. When the skin temperature of the middle site without a film (no-film condition) reached 33–34°C, measurements started. Control (no film condition) was included in every experiment for the purpose of setting a baseline of temperature increases.

3. Results

3.1 [Exp. 1] thermal effects of Cu-G composite films on a three-dimensional plastic surface

At the end of the 25-min heating, the cylinder surface temperature below the films was higher for the copper film condition than for the Cu-G film condition, where the film surface temperature was higher for the Cu-G film condition than for the copper film condition (Figure 4a and b). That is, the temperature difference between the surface of the cylinder and the surface of films was smaller for the Cu-G film condition than for the copper film condition (Figure 4a and b). MIDDLE cylinder surface temperatures beneath the films at the end of heating were 11.2 and 7.1°C higher when covered with copper film and Cu-G film, respectively, than for no-film condition (Figure 4a). The difference in the MIDDLE surface temperatures between the cylinder and copper film was 8.3°C at the end of heating, while the difference for the Cu-G film condition was 0.2°C (Figure 4b). UPPER and LOWER cylinder surface temperatures were lower than MIDDLE in all conditions (Figure 4c).

3.2 [Exp. 2] thermal effects of Cu-G composite films on the human-skin analogue

At air temperatures of 10 and 25°C, MIDDLE skin temperature was higher for the Cu-G film condition than for the copper film condition at the end of heating and heating-off (Figure 5, Table II). At the end of 30-min heating, MIDDLE skin temperatures for the copper and Cu-G film condition were 7.3 and 9.6°C higher than for the no-film condition at 10°C air temperature (Table II). At air temperature 25°C, those temperature differences were 6.9°C for the copper condition and 9.6°C for the Cu-G film condition. Even during the heating-off, MIDDLE skin temperatures were higher for the both film conditions than for the control (Table II). When exposed to an air temperature of 35°C, differences in the MIDDLE temperature between both film conditions were smaller when compared to those at the lower air temperatures (Table II). The pig-skin temperatures were not evenly distributed for the end of 30-min heating or for heating-off at the air temperatures of 10 and 25°C (Figure 5, Table II). Rather, transferred heat was accumulated on the heated section and the skin temperatures of the section remained the highest throughout the experiment in all three film conditions. Heat accumulation in MIDDLE was the most significant for the Cu-G film condition at the end of heating and the tendency lasted during the heating-off period (Figure 5). There were no remarkable differences between the three film conditions in the other skin sections, which were not directly heated.

		T_{air} of 10, 25, and 35°C		
	No film on the pig skin	Copper film on the pig skin	Cu-G film on the pig skin	Conditions (n)
No air trapped (flat)	0 layer	1 layer	1 layer	9
Air trapped in the middle (curved)	V1 (3.9 cm^3 in volume)	1, 2, 3, and 4 layers	1, 2, 3, and 4 layers	96
	V2 (7.9 cm^3)	1, 2, 3, and 4 layers	1, 2, 3, and 4 layers	
	V3 (17.7 cm^3)	1, 2, 3, and 4 layers	1, 2, 3, and 4 layers	
	V4 (23.6 cm^3)	1, 2, 3, and 4 layers	1, 2, 3, and 4 layers	
Total experimental conditions				105

Table I.
A total of 105 combinations of experimental factors in Experiment 3

Heating period	Temperature (°C)	No film	Copper film	CG film
End of heating (25 min)	Average cylinder surface	32.1	39.3	37.1
	Average film surface	-	35.0	37.1
	MIDDLE cylinder surface temperature difference from No film	-	11.2	7.1
End of heating-off (30 min)	Average cylinder surface	31.4	38.3	36.6
	Average film surface	-	34.5	36.5
	MIDDLE cylinder surface temperature difference from No film	-	10.6	7.3

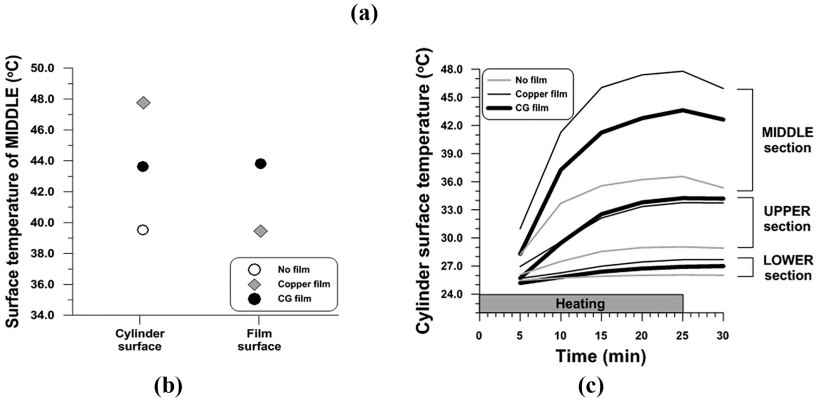

Figure 4.
[Exp. 1] Surface temperature of the cylinder and the films at an air temperature of 25°C (a), MIDDLE section temperatures on the cylinder and the films at the end of heating (b), MIDDLE, UPPER, LOWER section cylinder temperatures for 30 min of the heating protocol (c)

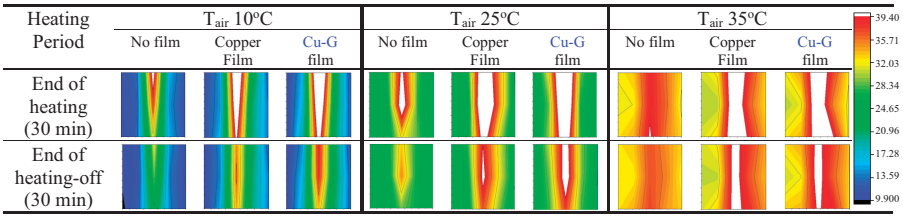

Figure 5.
[Exp. 2] Temperature distribution on the skin at the end of 30-min heating and 30-min after heating off at the air temperatures of 10, 25, and 35°C

3.3 [Exp. 3] thermal effects of Cu-G composite films with trapped air on human-skin analogue

Based on the results of the second experiment, we designed Experiment 3 to investigate heat accumulation inside the Cu-G film with various types of air gaps. Flat film conditions forming no air gap inside the film were first tested before changing the experimental system design that incorporated different conditions of air gaps. Results from the flat film conditions with no air gap for the third experiment showed a similar tendency (Figure 6a) to Exp. 2. That is, the pig-skin temperatures with flat copper or Cu-G films tended to be higher than the control, and the temperature for the Cu-G film condition was also inclined to be higher than for the copper condition in all the three air-temperature conditions. Temperature differences between the three conditions (no film, copper flat film, and Cu-G flat film) were the most remarkable at

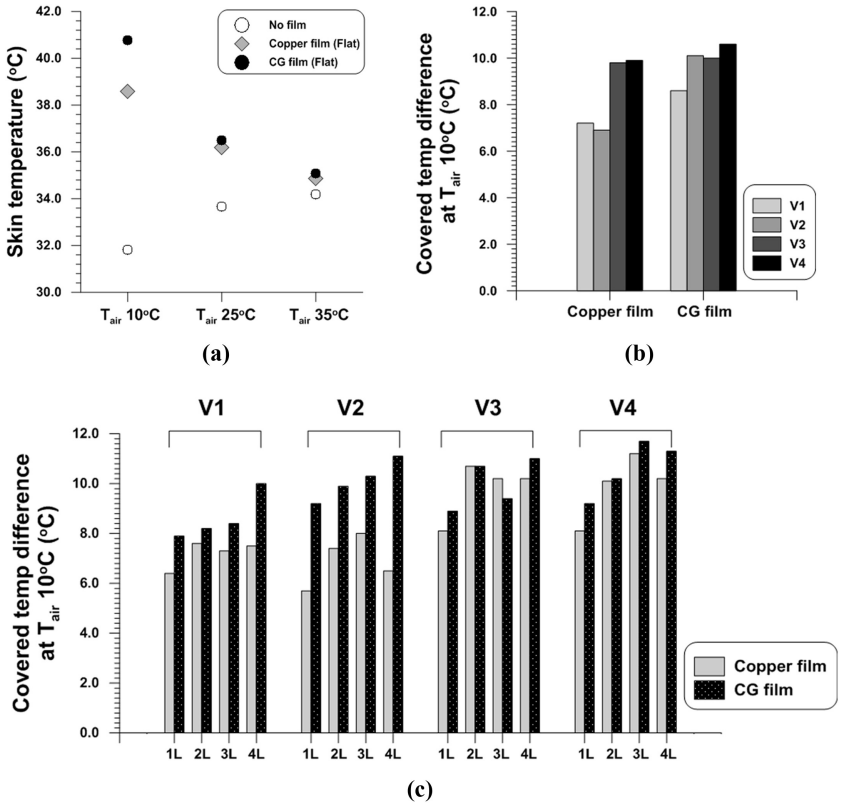

Figure 6.
[Exp. 3] Skin temperature in flat conditions at air temperatures of 10, 25, 35°C (a), covered temperature difference in curved conditions at the air temperature of 10°C (b), (c). All temperature data were obtained after 60 min of heating

10°C air temperature. Then, we tested the curved film conditions with varying air gap volumes and the number of film layers. The pig-skin temperatures in those conditions were expressed as "air-gap covered temperature difference," to represent the amount of increased temperature due to the air gap covering the skin beneath the films. This was calculated by subtracting the MIDDLE pig-skin temperature for the no-film condition from the copper or Cu-G film condition.

During the 60-min heating on the hot plate, air-gap-covered temperature difference gradually increased and the maximum value was 11.7°C at T_{air} 10°C (condition: Cu-G film condition, volume 4_23.6 cm^3, triple layers) (Figure 6c) (Table AI). The air-gap-covered temperature difference was on average 1.3°C and reached a maximum of 4.6°C higher for the Cu-G condition than for the copper condition (Figure 6c). Effects of trapped air volume and the number of film layers on the pig-skin temperatures were the most remarkable at the 10°C air temperature. For an average of 1–4 layers, larger trapped air volumes resulted in higher temperature differences at the end of heating for both copper condition (V1: 7.2°C, V2: 6.9°C, V3: 9.8°C, V4: 9.9°C) and Cu-G film condition (V1: 8.6°C, V2: 10.1°C, V3: 10.0°C, V4: 10.6°C) (Figure 6b). In each air gap volume condition, air-gap-covered temperature difference was the lowest with one layer of film (Figure 6c). At 25°C air temperature, thermal effects of air gap volume and the number of film layers were less significant compared to air temperature of 10°C, with averaged copper- or Cu-G-covered temperature difference at the end of heating of 2.5 and 2.6°C, respectively (Table AII). When exposed to 35°C air temperature, no significant thermal effects from air gap or film layers appeared (Table AIII).

Table II.
[Exp. 2] Regional average skin temperatures at the air temperature of 10, 25, and 35°C

			No film Surface section					Copper film Surface section					Cu-G film Surface section				
Air temp.	Heating	min[a]	*L2*[b]	*L1*[b]	*M*[b]	*R1*[b]	*R2*[b]	*L2*	*L1*	*M*	*R1*	*R2*	*L2*	*L1*	*M*	*R1*	*R2*
10°C	On	10	11.9	13.6	35.2	15.4	12.3	12.0	14.6	38.2	18.7	13.2	10.0	15.0	39.2	17.7	11.4
		30	10.7	12.6	*36.9*	15.3	11.3	11.0	15.3	*44.2*	21.8	13.3	10.3	17.1	*46.5*	22.4	11.9
	Off	40	10.4	12.6	36.2	15.2	11.1	10.7	15.4	43.7	22.4	13.5	10.3	17.5	46.4	23.3	12.0
		60	9.9	11.9	*28.1*	14.0	10.6	10.2	14.7	*35.2*	20.9	13.2	10.1	16.1	**37.2**	21.9	12.0
25°C	On	10	22.1	23.1	36.2	25.3	22.5	22.1	23.0	40.2	29.5	22.9	22.4	26.0	42.0	24.8	22.6
		30	22.5	24.1	*38.6*	28.0	23.1	22.7	25.2	*45.5*	33.5	24.1	23.3	30.0	*48.2*	27.8	23.9
	Off	40	22.6	24.1	37.9	28.1	23.1	22.9	25.8	45.0	33.9	24.4	23.5	30.7	47.7	28.6	24.4
		60	22.6	23.7	*32.5*	26.5	23.1	23.2	25.7	*38.9*	31.0	24.5	23.8	29.4	*40.5*	28.6	24.9
35°C	On	10	31.1	31.8	37.8	34.5	30.7	30.2	30.7	38.8	33.7	30.3	30.2	31.3	38.5	33.4	29.8
		30	32.1	33.1	39.1	35.9	32.2	30.8	31.9	43.3	37.5	33.0	31.6	33.2	42.9	37.5	31.8
	Off	40	32.3	33.3	39.0	35.9	32.5	30.9	32.0	43.5	38.1	33.7	31.9	33.5	43.1	38.1	32.4
		60	32.4	33.2	37.1	35.0	32.6	31.0	31.9	40.6	37.4	34.1	32.2	33.2	40.3	37.5	33.1

4. Discussion

The present study has significance in that it evaluated thermal effects of copper-graphene composite film in emulated next-to-skin microclimate environments. Pig skin used to imitate the human skin was heated to reproduce temperature distribution of the human skin in global and local regions. Differential effects of clothing microclimate characteristics such as air gap volume and film layers were tested. Last but not least, by exposing the experimental system to three typical ambient temperatures (10, 25, and 35°C), the present study incorporated heat exchange between the human skin and environment into the experimental system.

4.1 Heat accumulation inside the copper-graphene composite films and copper films

Skin temperatures of the heated sites by the heating system or the hot plate were higher in Cu-G and Copper film conditions than in no-film conditions. Copper can be used as a layer of thermoregulatory textiles playing an insulating role since it has low emissivity due to its high reflectivity as other metals also generally do (Hsu *et al.*, 2017). Therefore, it is logical to understand that the metal film and the substrate used as a clothing layer in the present study were effective in preserving heat transferred from the heat source, reflecting infrared radiation back to the skin (Hsu *et al.*, 2015). In addition, although the skin temperatures of the nonheated sites of Cu-G film and copper film tended to be higher than for no-film condition, heat distributing effects of Cu-G and copper film were not dramatic, not compensating for the heat accumulation (Exp. 2). The results seem to go against the general applicability of copper or graphene as a heat dissipator, that is, having good in-plane thermal conductivity, for electronic devices.

However, this may be explained as follows. First of all, the heat source in the present study was not placed directly on the film layers but beneath the skin to simulate heat exchange in a clothing microclimate. Human-skin temperature is regulated by a combination of complex heat transfer actions such as evaporation, conduction, convection, and radiation (Wissler, 1961). It may thus not be enough to understand the heat transfer in the microclimate only in terms of heat conduction, just as in thermal management of electronic devices (e.g. Gao *et al.*, 2013). Second, improved thermal conductivity obtained by coating the copper film with a graphene monolayer on both sides (Goli *et al.*, 2014) may not be enough to spread the heat along the surface. Suspended graphene's high reported thermal conductivity of 3,000–5000 $W \cdot m^{-1} \cdot K^{-1}$ can degrade to 600 $W \cdot m^{-1} \cdot K^{-1}$ when contact is made with a substrate, owing to graphene–substrate coupling and phonon scattering across the interface (Seol *et al.*, 2010). Despite the limited thermal conductivity of supported graphene, its application to such things as copper-based composites results in improved mechanical properties (Balandin, 2011), including their friction coefficients, wear rates, and mechanical strengths (Chen *et al.*, 2016; Chmielewski *et al.*, 2016; Dutkiewicz *et al.*, 2015).

4.2 Heat accumulation inside the copper-graphene composite films at a low ambient temperature

Heat accumulation was more significant in Cu-G film condition than in Copper film condition when applied to the global (Exp. 2) and local skin regions (Exp. 3), at 10°C air temperature. Though not directly measured, the fact that Cu-G film insulated the skin more in colder environments might indicate that radiant heat loss was largely reduced; this loss should be proportional to the temperature difference between the skin and ambient temperature (Bennett *et al.*, 1994) and typically accounts for approximately 60 percent of heat loss in human body at rest (Ulrich and Rathlev, 2004). Compared to the bare skin, skin temperature under Cu-G film was up to 11.7°C higher after the bottom skin surface started being heated with the hot plate, when exposed to 10°C of air. More salient thermal effects of

Cu-G film in the low ambient temperature can be attributed to higher set temperature of the heating system or the hot plate for the purpose of reaching the mean skin temperature of the human body in a comfort range. When the human body is exposed to cold, heat production, or thermogenesis, is induced by shivering in skeletal muscles and nonshivering thermogenesis in the brown adipose tissue (Janský, 1973), which is reflected in the higher set temperature of the current study. Taken together, the results of the present study indicate that applying Cu-G film as a clothing layer may have a positive impact on conserving the body heat, despite the larger temperature gradient between the body and a cold environment. The possible reason for the superior heat accumulation effect from an extremely thin layer of graphene on the copper-based film is worthy to be further explored.

Reduced heat dissipation at a low ambient temperature is significant for the human body in terms of decreasing the risk of cold-related injuries and illnesses. Even though the human body can control physiological responses to cold exposure and regulate body temperatures through the hypothalamus, this compensatory mechanism is finite (Tikuisis *et al.*, 2002). As the human capacity to produce heat is limited, certain situations that facilitate body heat loss can trigger the onset of hypothermia, which is classically defined as a body core temperature below 35°C and has deleterious impacts on renal, cardiac, and central nervous systems (Ulrich and Rathlev, 2004). To prevent hypothermia, passive or active warming is commonly applied because changes in skin temperatures can affect core-body temperature regulation. According to Just *et al.* (1993), elevating mean skin temperature by 3.4°C through warming the chest and the shoulders was effective in reducing decrement in body core temperature. In a study by Bennett *et al.* (1994), which compared the effectiveness of passive and active skin warming for preventing hypothermia, however, it was reported that passive warming is only efficient for keeping the mean skin temperatures in normal ranges not for maintaining body core temperature. Therefore, the insulation of Cu-G film when applied as a clothing layer can appear more efficient when used with an active warming method.

4.3 Effects of air gap volume and film layers on heat accumulation inside copper-graphene composite films

Having very low thermal conductivity of 0.026 $W \cdot m^{-1} \cdot K^{-1}$, stagnant air can be a good insulator as long as the trapped air is not too wide and thick for natural air convection to occur inside clothing (Song, 2007). Among the factors affecting clothing thermal insulation, stagnant air layers have been reported to be one of the most significant (Morris, 1953). The results from Exp. 3 in the present study, showing the relationship between trapped air volume and heat accumulation inside Cu-G film, therefore, are consistent with previous studies. One interesting finding is that the maximum number of film layers was not necessarily related to the highest skin temperature under Cu-G film, though it was evident that more than two layers had more beneficial thermal effects than a single layer. As the multiple film layers all formed the same-shape air gap in each condition and overlapped, superior heat concentration effect of multiple Cu-G film layers is not likely to be associated with difference in air gap volume. Rather, multiple insulating layers may be more linked to reducing radiant heat loss. Taken together, the results suggest that there can be optimal combinations of skin–clothing air gap volume and number of layers for the development of thermal-protective clothing using Cu-G films.

4.4 Limitation and suggestions

Thermal effects of the copper-graphene composite films found in the current study should be further investigated and supported by lab-scale experiments examining thermal properties of

graphene itself. There is a problem in applying a metal-graphene composite film to clothing as it is, due to its low air and vapor permeability. As such properties must be avoided in order to prevent too impaired thermal comfort, textile engineers should be attentive when to utilize the possible insulating effects of copper-graphene composite materials. We also suggest further examination of thermal effects of supported graphene in the microclimate using other kinds of substrates. Last but not least, one should be careful in interpreting the results of the present study as we used a human-skin "analogue." Although pig skin has been commonly used as a substitute for human skin in many studies, warmed pig skin is not exactly the same as the human skin whose temperature is controlled by complex thermoregulatory mechanisms.

5. Conclusions

We evaluated thermal effects of copper-graphene composite films on humin-skin analogue varying the characteristics of the microclimate between the skin and clothing, in cold, mild, and hot environments. Emulating cutaneous vascular system as well as different types of air gaps inside the clothing, the main experiments in the present study suggested that especially in cold environments, the human-skin analogue can be insulated more when covered with Cu-G films: heat transferred from the heating system did not spread along the film surfaces, rather being accumulated in the heated area. In addition, we also discovered that the air gap volumes seemed to affect heat accumulation under the films, which appeared to be less related to the number of the film layers. These findings indicate that (1) it is necessary to match test environments and real settings of applications to explore how certain thermal characteristics of Cu-G films will affect the skin; (2) efforts to optimize the air gap conditions seem imperative. Insulating effects of Cu-G films shown by the current studies may be applicable to cold-protective clothing, though the results should be carefully construed and be further demonstrated.

References

Bae, S., Kim, H., Lee, Y., Xu, X., Park, J.S., Zheng, Y., Balakrishman, J., Lei, T., Kim, H., Song, Y., Kim, Y.J., Kim, K., Ozyilmza, B., Ahn, J.H., Hong, B. and Iijima, S. (2010), "Roll-to-roll production of 30-inch graphene films for transparent electrodes", *Nature Nanotechnology*, Vol. 5 No. 8, pp. 574-578.

Balandin, A.A. (2011), "Thermal properties of graphene and nanostructured carbon materials", *Nature Materials*, Vol. 10 No. 8, pp. 569-581.

Bennett, J., Ramachandra, V., Webster, J. and Carli, F. (1994), "Prevention of hypothermia during hip surgery: effect of passive compared with active skin surface warming", *British Journal of Anaesthesia*, Vol. 73 No. 2, pp. 180-183.

Chen, F., Ying, J., Wang, Y., Du, S., Liu, Z. and Huang, Q. (2016), "Effects of graphene content on the microstructure and properties of copper matrix composites", *Carbon*, Vol. 96, pp. 836-842.

Chmielewski, M., Michalczewski, R., Piekoszewski, W. and Kalbarczyk, M. (2016), "Tribological behaviour of copper-graphene composite materials", *Key Engineering Materials*, Vol, 674, pp. 219-224.

Dutkiewicz, J., Ozga, P., Maziarz, W., Pstruś, J., Kania, B., Bobrowski, P. and Stolarska, J. (2015), "Microstructure and properties of bulk copper matrix composites strengthened with various kinds of graphene nanoplatelets", *Materials Science and Engineering: A*, Vol. 628, pp. 124-134.

Gao, Z., Zhang, Y., Fu, Y., Yuen, M.M. and Liu, J. (2013), "Thermal chemical vapor deposition grown graphene heat spreader for thermal management of hot spots", *Carbon*, Vol. 61, pp. 342-348.

Goli, P., Ning, H., Li, X., Lu, C.Y., Novoselov, K.S. and Balandin, A.A. (2014), "Thermal properties of graphene–copper–graphene heterogeneous films", *Nano Letters*, Vol. 14 No. 3, pp. 1497-1503.

Hsu, P.C., Liu, C., Song, A.Y., Zhang, Z., Peng, Y., Xie, J., Liu, K., Wu, C.L., Catrysse, P.B., Cai, L., Zhai, S., Majumdar, A., Fan, S. and Cui, Y. (2017), "A dual-mode textile for human body radiative heating and cooling", *Science Advances*, Vol. 3 No. 11, e1700895.

Hsu, P.C., Liu, X., Liu, C., Xie, X., Lee, H.R., Welch, A.J., Zhao, T. and Cui, Y. (2015), "Personal thermal management by metallic nanowire-coated textile", *Nano Letters*, Vol. 15 No. 1, pp. 365-371.

Ito, Y., Tanabe, Y., Sugawara, K., Koshino, M., Takahashi, T., Tanigaki, K., Aoki, H. and Chen, M. (2018), "Three-dimensional porous graphene networks expand graphene-based electronic device applications", *Physical Chemistry Chemical Physics*, Vol. 20 No. 9, pp. 6024-6033.

Janskÿ, L. (1973), "Non-shivering thermogenesis and its thermoregulatory significance", *Biological Reviews*, Vol. 48 No. 1, pp. 85-132.

Just, B., Trëvien, V., Delva, E. and Lienhart, A. (1993), "Prevention of intraoperative hypothermia by preoperative skin-surface warming", *Anesthesiology*, Vol. 79 No. 2, pp. 214-218.

Kim, K., Zhao, Y., Jang, H., Lee, S., Kim, J., Kim, K., Ahn, J.H., Kim, P., Choi, J.Y. and Hong, B. (2009), "Large-scale pattern growth of graphene films for stretchable transparent electrodes", *Nature*, Vol. 457 No. 7230, pp. 706-710.

Kim, D., Yoo, J., Hwang, H., Lee, J., Yun, S., Park, M., Lee, M., Choi, S., Kwon, S., Lee, S., Kwon, S.H., Kim, S., Park, Y., Kinoshita, M., Lee, Y.H., Shin, S., Paik, S., Lee, S., Lee, S., Hong, B. and Ko, H. (2018a), "Graphene quatum dots prevent α-synucleinopathy in Parkinson's disease", *Nature Nanotechnology*, Vol. 13 No. 9, pp. 812-818.

Kim, S., Shin, D., Choi, Y., Rho, H., Park, M., Moon, B., Kim, Y., Lee, S.K., Lee, D., Kim, T.W., Lee, S., Kim, K., Hong, B. and Bae, S. (2018b), "Ultrastrong Graphene-copper core-shell wires for high-performance electrical cables", *ACS Nano*, Vol. 12 No. 3, pp. 2803-2808.

Lee, B., Kang, J.H., Jo, I., Shin, D. and Hong, B. (2016), "Graphene-catalyzed photoreduction of dye molecules revealed by graphene enhanced Raman spectroscopy", *Physical Chemistry Chemical Physics*, Vol. 18 No. 5, pp. 3413-3415.

Lin, S.Y., Zhang, T.Y., Lu, Q., Wang, D.Y., Yang, Y., Wu, X.M. and Ren, T.L. (2017), "High-performance graphene-based flexible heater for wearable applications", *RSC Advances*, Vol. 7 No. 43, pp. 27001-27006.

Mao, J., Iocozzia, J., Huang, J., Meng, K., Lai, Y. and Lin, Z. (2018), "Graphene aerogels for efficient energy storage and conversion", *Energy and Environmental Science*, Vol. 11 No. 4, pp. 772-799.

Morris, G.J. (1953), "Thermal properties of textile materials", *Journal of the Textile Institute Transactions*, Vol. 44 No. 10, pp. T449-T476.

Parsons, K. (2014), *Human Thermal Environments: The Effects of Hot, Moderate, and Cold Environments on Human Health, Comfort, and Performance*, CRC press, New York.

Seol, J.H., Jo, I., Moore, A.L., Linsay, L., Aitken, Z.H., Pettes, M.T., Li, X., Yao, Z., Huang, R., Broido, D., Mingo, N., Ruoff, R.S. and Shi, L. (2010), "Two-dimensional phonon transport in supported graphene", *Science*, Vol. 328 No. 5975, pp. 213-216.

Shin, S., Choi, H.H., Kim, Y.B., Hong, B. and Lee, J.Y. (2017), "Evaluation of body heating protocols with graphene heated clothing in a cold environment", *International Journal of Clothing Science and Technology*, Vol. 29 No. 6, pp. 830-844.

Song, G. (2007), "Clothing air gap layers and thermal protective performance in single layer garment", *Journal of Industrial Textiles*, Vol. 36 No. 3, pp. 193-205.

Sullivan, T.P., Eaglstein, W.H., Davis, S.C. and Mertz, P. (2001), "The pig as a model for human wound healing", *Wound Repair and Regeneration*, Vol. 9 No. 2, pp. 66-76.

The Nobel Prize (2010), *Graphene – the Perfect Atomic Lattice*, 5 October.

Tikuisis, P., Eyolfson, D.A., Xu, X. and Giesbrecht, G.G. (2002), "Shivering endurance and fatigue during cold water immersion in humans", *European Journal of Applied Physiology*, Vol. 87 No. 1, pp. 50-58.

Ulrich, A.S. and Rathlev, N.K. (2004), "Hypothermia and localized cold injuries", *Emergency Medicine Clinics of North America*, Vol. 22 No. 2, pp. 281-298.

Wissler, E.H. (1961), "Steady-state temperature distribution in man", *Journal of Applied Physiology*, Vol. 16 No. 4, pp. 734-740.

Zhang, P., Gong, R.H., Yanai, Y. and Tokura, H. (2002), "Effects of clothing material on thermoregulatory responses", *Textile Research Journal*, Vol. 72 No. 1, pp. 83-89.

Corresponding author
Joo-Young Lee can be contacted at: leex3140@snu.ac.kr

Appendix

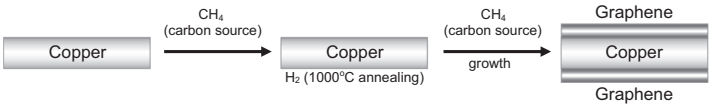

Figure A1.
Synthesis process of the copper-graphene composite film

Table AI.
[Exp. 3] MIDDLE cover temperature difference at the air temperature of 10°C

	V1 (3.9 cm^3)				V2 (7.9 cm^3)				V3 (17.7 cm^3)				V4 (23.6 cm^3)			
	1L	2L	3L	4L	1L	2L	3L	4L	1L	2L	3L	4L	1L	2L	3L	4L
Copper film condition at T_{air} 10°C																
Time (min) 10	5.7	6.6	6.0	6.1	5.1	6.5	6.6	5.2	7.6	9.7	9.3	9.2	7.3	9.0	9.9	9.1
30	6.0	7.1	6.8	7.0	5.2	6.9	7.4	6.0	7.8	10.1	9.7	9.7	7.7	9.6	10.5	9.6
60	6.4	7.6	7.3	7.5	5.7	7.4	8.0	6.5	8.1	10.7	10.2	10.2	8.1	10.1	11.2	10.2
Cu-G film condition at T_{air} 10°C																
Time (min) 10	6.3	7.4	6.2	6.9	7.1	7.6	7.5	8.3	6.8	8.1	7.1	7.9	7.0	7.5	8.7	8.3
30	7.4	8.3	7.4	8.8	8.2	8.9	9.1	9.9	7.8	9.4	8.4	9.7	8.1	8.9	10.3	10.0
60	7.9	8.2	8.4	10.0	9.2	9.9	10.3	11.1	8.9	10.7	9.4	11.0	9.2	10.2	11.7	11.3

		V1 (3.9 cm^3)				V2 (7.9 cm^3)				V3 (17.7 cm^3)				V4 (23.6 cm^3)			
		1L	2L	3L	4L	1L	2L	3L	4L	1L	2L	3L	4L	1L	2L	3L	4L
Copper film condition at T_{air} 25°C																	
Time (min)	10	2.2	2.3	2.1	1.8	2.8	2.6	2.4	2.4	2.0	2.9	2.0	1.9	2.8	3.1	2.6	2.7
	30	1.8	2.1	2.1	2.0	2.3	2.2	2.2	2.3	2.3	3.3	2.8	2.9	2.8	3.2	3.0	3.2
	60	1.7	2.1	2.1	1.9	2.2	2.0	2.1	2.3	2.3	3.4	3.0	3.0	2.8	3.3	3.1	3.3
Cu-G film condition at T_{air} 25°C																	
Time (min)	10	1.8	2.3	2.2	1.5	2.7	2.9	2.3	2.2	2.0	2.0	1.6	1.9	2.4	2.3	2.3	2.1
	30	1.9	2.5	2.5	1.9	2.8	3.0	2.6	2.2	2.2	2.3	2.1	2.5	2.5	2.7	2.8	2.7
	60	1.9	2.6	2.6	2.0	2.9	3.2	2.7	2.3	2.5	2.5	2.5	2.9	2.7	2.9	3.1	3.0

Table AII.
[Exp. 3] MIDDLE cover temperature difference at the air temperature of 25°C

Table AIII.
[Exp. 3] MIDDLE cover temperature difference at the air temperature of 35°C

		V1 (3.9 cm^3)				V2 (7.9 cm^3)				V3 (17.7 cm^3)				V4 (23.6 cm^3)			
		1L	2L	3L	4L	1L	2L	3L	4L	1L	2L	3L	4L	1L	2L	3L	4L
Copper film condition at T_{air} 35°C																	
Time (min)	10	0.5	0.4	0.1	0.0	0.6	0.3	0.3	0.2	0.4	0.4	0.1	0.2	0.6	0.5	0.3	0.2
	30	0.6	0.6	0.3	0.2	0.7	0.6	0.5	0.4	0.5	0.6	0.3	0.5	0.6	0.6	0.6	0.4
	60	0.6	0.7	0.4	0.3	0.7	0.6	0.5	0.5	0.5	0.7	0.4	0.5	0.6	0.6	0.6	0.5
Cu-G film condition at T_{air} 35°C																	
Time (min)	10	0.2	0.4	−0.1	−0.1	0.4	0.3	0.1	0.0	0.2	0.3	−0.2	−0.1	0.3	0.2	0.0	−0.1
	30	0.3	0.6	0.2	0.3	0.5	0.4	0.4	0.2	0.3	0.5	0.1	0.2	0.3	0.3	0.2	0.1
	60	0.3	0.6	0.2	0.4	0.4	0.4	0.4	0.3	0.3	0.5	0.2	0.2	0.3	0.4	0.3	0.2